Differential energy-loss cross sections for ionization of atomic hydrogen by 25–200-keV protons*

J. T. Park, J. E. Aldag, J. M. George, and J. L. Peacher
Department of Physics, University of Missouri-Rolla, Rolla, Missouri 65401

J. H. McGuire†
Department of Physics, Kansas State University, Manhattan, Kansas 66506
(Received 13 May 1976)

Ionization continuum cross sections, differential in energy loss, have been determined from the energy-loss spectra of 25-, 50-, 75-, 145-, and 200-keV protons scattered from atomic hydrogen. The theoretical differential cross sections in the Glauber and Born approximations that are presented show that the theory and the experimental results for 200-keV proton impact agree very well, but below 200 keV there are differences. These differences, which are more pronounced at the lower projectile energies, may be explained in terms of charge transfer to the continuum, which is not treated in our Born and Glauber calculations of direct Coulomb ionization. The total ionization cross sections obtained by integrating the differential cross sections are in reasonable agreement with ionization cross-section measurements that have been obtained from crossed-beam experiments.

INTRODUCTION

Numerous measurements have been made of both the total cross sections for ionization and the energy distribution of the ejected electrons from multielectron atoms; however, there have been only two measurements made of the total cross section for ionization of atomic hydrogen by protons.[1,2] No measurements of the energy distribution of the ejected electrons for this fundamental collision system have been made, because direct measurement is very difficult.[3] To obtain accurate cross sections, one must place precision apparatus in a field-free region, and the collection geometry as well as the detector's efficiency must be carefully measured. The results have to be corrected for absorption of electrons between the collector and detector, for ion beam neutralization, residual gas, dead-time losses, and for variation of the detector's efficiency with electron energy. Also, the usual correction has to be made for target density variations.[3] Even with these corrections and the use of excessive care in experimental technique, many difficulties are encountered in handling electrons with energies less than 5 eV.[4] In addition, when an atomic hydrogen target is used, the problems are compounded by the requirement of a dissociating furnace and the use of crossed-beam techniques.

These problems, as described below, have been solved through an analysis of the energy that is lost in the collision of an incident proton rather than of the energy that is gained by an ejected electron.[5-11] Because an incident proton moves at high velocity, it is not greatly perturbed by small residual magnetic fields. It is, therefore, possible to use a transmission target furnace as the source of atomic hydrogen. The energy-loss technique also provides one with the advantage of being able to measure the energy losses that correspond to the ejected electrons that possess low energy.

In this paper, the first measurement of a differential energy-loss cross section for the ionization continuum of atomic hydrogen is recorded. For the large impact parameters, which dominate this scattering cross section, the energy lost to the nucleus is very small compared to the energy transferred to the electron and can be neglected. Therefore, if one assumes that there are no unknown inelastic processes that give the same energy loss as ionization, the differential energy-loss cross sections reported here are essentially the same as the differential cross sections for electrons ejected at all angles.

Theoretical studies of the ejected electron energy distribution are limited in number. Most work that has been done involves the Born approximation,[12] which is supposed to be valid at high energies, and the classical binary encounter model.[13] Born approximation calculations of ejected electron energy spectra are included in the present paper.

The Glauber treatment of collision processes in many cases has been proven to be superior to the Born approximation treatment,[14-16] and the Glauber approximation calculations of cross sections for the excitation of atomic hydrogen by incident protons agree very well with measurements made in our laboratory.[5,17] Glauber calculations are pre-

sented herein for the ionization differential cross sections, $d\sigma/d\xi$, in which ξ is the energy lost by the projectile in the collision. Integration of these differential cross sections yields the total cross sections for ionization by proton impact of atomic hydrogen that was reported earlier by Golden and McGuire.[18] A comparison of these theoretical predictions with energy spectra observed by us delineates a breakdown of the Glauber theory for ionization by proton impact.

EXPERIMENTAL METHOD

The energy-loss spectrometer at the University of Missouri-Rolla and the general method employed in ion energy-loss spectrometry have been discussed in detail elsewhere.[5-11,17] In these measurements, the experimental arrangement is identical to that used to obtain cross sections for excitation by protons of atomic hydrogen.[5,17] The protons produced in a low-voltage discharge source are focused and mass-analyzed by a Wien filter. The protons are then accelerated and steered through a target furnace chamber. After traversing the scattering chamber, the protons pass through an exit collimator, and the transmitted beam is magnetically analyzed. Following this, the protons are decelerated by a well-defined potential, analyzed by a 127° electrostatic energy analyzer, and detected with a particle multiplier. Energy-loss spectra are obtained by increasing the potential difference between the accelerator and decelerator terminals ΔV. Whenever the increased potential energy compensates for a discrete energy loss in the proton-atomic hydrogen collision system, a peak is detected in the spectrum. The energy loss can be determined to an accuracy of ±0.03 eV.[8]

The experimental arrangement used when atomic hydrogen is the desired target has been discussed in Ref. 17. The atomic hydrogen target gas is formed in a high temperature furnace that is constructed of coaxial tungsten tubes. The proton beam is directed coaxially through the center of the furnace. The path length of the ion beam in the atomic hydrogen furnace is 10.2 cm. The furnace is differentially pumped using fast diffusion pumps.

The absolute density of the atomic hydrogen cannot be determined directly; however, if the pressure in the target furnace and the target temperature are fixed the density remains constant. As will be discussed below, the density is determined by a normalization procedure. The purity of the atomic hydrogen target is established from the energy-loss spectra. The energy-loss spectrum of each gas is unique and permits definite identification.

When the atomic hydrogen pressure in the hot furnace is raised to 0.54×10^{-3} Torr as determined by the normalization procedure discussed below, the pressure in the differential pumping region increases from 4×10^{-7} to 1×10^{-6} Torr. Even if this pressure increase in the differential pumping region is entirely due to molecular hydrogen formed by recombination, the total 8.8-cm path length in the differential pumping region would provide only 0.1% of the target particles provided by the atomic hydrogen in the furnace. This fact implies that the features observed in a energy-loss spectrum will be dictated by the constituency of the gas in the target furnace.

With the target furnace cold, the energy-loss spectrum of molecular hydrogen is obtained when the hydrogen gas is introduced into the target cell. The spectrum as a result of the Lyman α bands displays a broad peak at 12.5 eV. This spectrum starts at about 11.2 eV energy loss, reaches a peak at 12.5 eV, and decreases monotonically at higher energy losses. As the furnace is heated, the spectrum begins to change. A new peak at 10.2 eV energy loss that is attributed to the excitation of atomic hydrogen to the $n=2$ state appears and increases while the peak at 12.5 eV changes shape and decreases. However, in this spectrum, the peak near 12.5 eV is now primarily due to the excitation of atomic hydrogen to the $n=3$ and $n=4$ states. The monotonically decreasing tail is due to excitations of higher discrete states and the ionization continuum. The spectrum observed at high furnace temperatures is essentially the same as the averaged spectrum shown in Fig. 1.

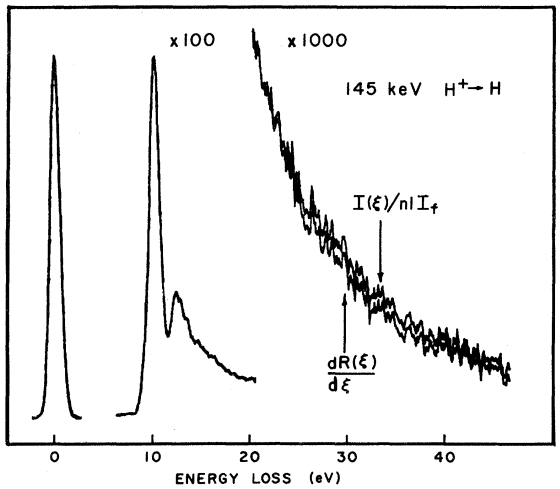

FIG. 1. Energy-loss spectrum for atomic hydrogen under proton bombardment. The data are shown with and without correction for multiple collision effects; see text.

The determination of the cross section for excitation to the $n=2$ state does not depend on the complete dissociation of the molecular hydrogen, because the 10.2 eV peak is well resolved from the molecular peak. However, the broad peak at 12.5 eV may contain a small contribution from the Lyman α bands of any residual molecular hydrogen in the furnace. As the furnace temperature is increased, the atomic hydrogen increases while the molecular hydrogen is depleted and the molecular contribution to the 12.5-eV energy-loss peak is reduced. The ratio of the peak at 10.2 eV to the peak at 12.5 eV can therefore be used as an indication of the amount of residual molecular hydrogen present in the target furnace. This ratio increases with temperature until it reaches a plateau. Raising the furnace temperature further does not make any observable changes in spectral shape indicating that the molecular hydrogen no longer makes a significant contribution to the spectrum. From these considerations, the molecular fraction is estimated to be no more than 3% and is probably less than 1% during the data acquisition period.

The limits on the molecular fraction estimated from the temperature and pressure conditions are not as reliable as those based on observations of the energy-loss spectra. This is because the temperature of the inside wall of the double-walled furnace during operation must be inferred from measurements of the temperature of the outer wall compared with measurements of the temperatures of both walls which were taken prior to the furnace installation. Using the temperature determined in this way and observing the energy-loss spectra, the ratio of the 10.2 peak to the 12.5 peak shows almost no additional change when the temperature of the furnace is increased above 2475°K. The temperature of the furnace was estimated to be about 2650°K during the experiment. With 0.54×10^{-3} Torr gas pressure in the furnace, the residual molecular hydrogen would be about 1% of the target gas. This is consistent with the more reliable measurement which used the energy-loss spectra.

DATA

The energy resolution of the system used in this experiment is 1.0 eV (see Fig. 1). Better energy resolution has been obtained in some previous experiments.[7] However, the requirements of this experiment for long term stability of the proton beam current dictated some concessions in ion source parameters which resulted in slightly poorer energy resolution.

At each impact energy, a spectrum is taken by recording the ion current at 0.1 eV intervals in energy loss. The measured pressure at the time of the reading is also recorded. Effects resulting from small differences between the set pressure and the measured pressure are corrected during the analysis of the data. These corrections are typically 2% or less. If the pressure correction to any data point exceeds 15%, the data run is automatically aborted. Typically six energy-loss spectra are obtained with gas in the target chamber, and six spectra are obtained without gas at each impact energy. The average of the spectra taken with no gas in the furnace is scaled to take into account the protons that are lost as a result of the charge changing effects and is then subtracted point by point from the average of the spectra that are obtained with gas in the chamber.

Consecutive sets of these energy-loss spectra are taken at various energies of the incident proton from 200 keV down to 25 keV and back up to 200 keV. The pressure and temperature in the target furnace are held constant during the entire series, thus the atomic hydrogen density in the furnace is also constant. This technique makes it possible to normalize the entire series of spectra to a theoretical cross section. (The normalization effectively determines the density of atomic hydrogen in the target furnace.)

While the probability that a proton will undergo a second inelastic collision is very small, the data are corrected for such secondary inelastic collisions. At large energy losses, the data may be the sum of single and multiple collision events; however, a proton undergoing two inelastic collisions would lose a minimum of 20.4 eV. Losses of energy less than this can only be due to single collision processes. The probability of a multiple inelastic collision can therefore be calculated from the data, and double collision contributions can then be subtracted from the data at large energy losses.

The corrected spectrum, $dR(\xi)/d\xi$, is a convolution of the energy resolution function, $\Phi(\xi)$, with the differential cross section for energy loss, $d\sigma(\xi)/d\xi$,

$$\frac{dR(\xi)}{d\xi} = \int \frac{d\sigma(\xi')}{d\xi'} \Phi(\xi - \xi')\, d\xi' \,. \tag{1}$$

The resolution function $\Phi(\xi)$ is determined from the unscattered beam energy profile. It essentially has the profile shown for the zero energy-loss peak and $\int \Phi(\xi)\, d\xi = 1$. For the purpose of determining the differential cross sections from the data, the corrected spectrum is given by

$$\frac{dR}{d\xi} = \frac{1}{nlI_f} I(\xi) - \frac{nl}{2} \int \frac{dR(\xi')}{d\xi'} \frac{d\sigma(\xi - \xi')}{d\xi'}\, d\xi' \,. \tag{2}$$

In this equation, l is the length of the collision chamber, n the atomic hydrogen density, I_f the total current obtained by integrating the elastic peak of the spectrum, which is centered at zero energy loss, and $I(\xi)$ the proton current measured at an energy loss ξ. The integral in this equation is the double collision correction. An ion which has lost an energy ξ' in a collision has a certain probability of undergoing a second collision with an energy loss of $\xi - \xi'$ to give a total energy loss of ξ.

To obtain the differential cross section, the composite differential cross section is assumed to have the form

$$\frac{d\sigma(\xi)}{d\xi} = \sum_n \sigma_n \delta(\xi - \xi_n) + \sum_m A_m \xi^{-m} . \qquad (3)$$

The term σ_n is the cross section for excitation to the nth discrete state. The summation over n describes excitation to the $n=2, 3, 4$ states at the well-known transition energies, ξ_n, with the δ function representing the very narrow line shape. The second term, $\sum_m A_m \xi^{-m}$, is a series that is used to represent the continuum and discrete states that are so closely spaced as to appear as a continuum in the spectrum. The coefficient A_m is equal to zero if $\xi < \xi_I$. The term ξ_I is the energy of the first state not explicitly included in the summation over n.

No discontinuity in the spectrum is observed at the ionization potential indicating a smooth transition from discrete to continuum states. It is impossible to specifically include all discrete states and the calculated cross sections for these states become meaningless once the separation of the states is less than the 0.1-eV step size. Within these limits changing the number of discrete states specifically considered did not significantly change the low-energy discrete states or the A_m coefficients.

The exponents m are chosen to fit the high-energy tail. The A_m and σ_m coefficients in Eq. (3) are obtained by a least-squares fit, which minimizes D;

$$D = \sum_i \left(\int \frac{d\sigma(\xi)}{d\xi} \Phi(\xi_i - \xi)\, d\xi - \frac{dR(\xi_i)}{d\xi} \right)^2 \qquad (4)$$

in which the discrete ξ_i are the energy-loss values at the data points on the spectrum. At some energy-loss values the continuum and discrete states both contribute to the spectrum. Thus, the procedure fits both discrete and continuum states simultaneously.

The above equations for $d\sigma/d\xi$ are solved by an iteration that starts with the measured spectrum. $dR/d\xi$ is set equal to $(1/nlI_f)I(\xi)$, and the equations are iterated until self-consistency is obtained for $d\sigma/d\xi$.

Because the experiment is performed under essentially single-collision conditions, the correction resulting from double collisions is very small as can be seen from Fig. 1. Figure 1 shows the spectrum with and without the double-collision correction.

Figure 2 shows the continuum of the corrected spectra, $dR/d\xi$, and the calculated differential cross sections, $d\sigma/d\xi = \sum_m A_m \xi^{-m}$ for $\xi > 13.6$ eV. The data are normalized to the Born approximation calculation of the cross section for excitation of atomic hydrogen to the $n=2$ state by 200-keV protons.[5,17] The normalization effectively determines the absolute atomic hydrogen density in the target furnace. This normalization determines the normalization of the data at all other impact energies, because the relative normalization is maintained

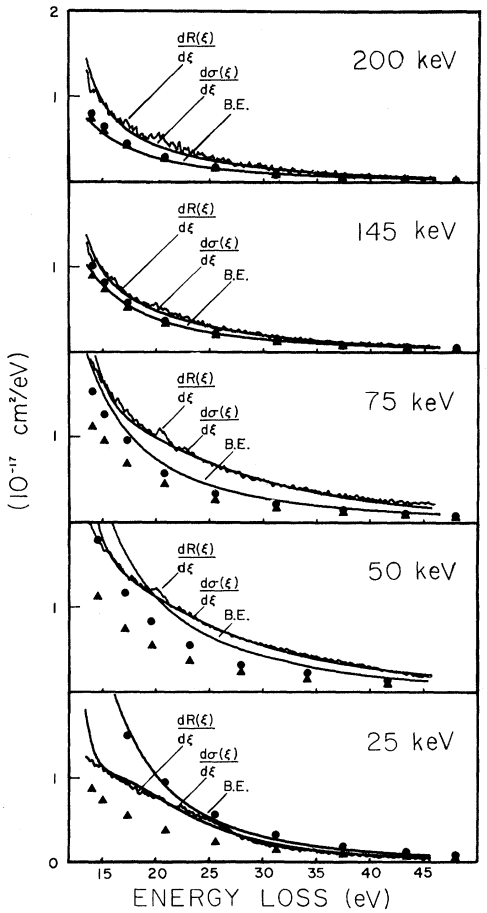

FIG. 2. Cross sections differential in energy loss for the proton impact ionization continuum of atomic hydrogen. B.E. is the binary encounter calculation of Garcia (Ref. 13). The solid circles are our Born approximation calculations. The solid triangles are our Glauber approximation calculations; see text.

by the procedures used in the data taking and analysis.

Table I gives values of the coefficients obtained in the fitting process. The table is included to permit the reader to reproduce the data. It must be noted that the choice of the exponents is somewhat arbitrary and equally good fits could be obtained with other exponents and coefficients. A satisfactory fit to the data could not be obtained by using a single exponent.

THEORY

While there is no rigorous and complete quantum theory of ionization by charged particles of atomic hydrogen, there are a number of approximate calculations. These include both exact[19] and approximate[13] classical calculations as well as quantum approximations based primarily on the Born[12,20-22] approximation, which is generally considered valid at high projectile velocities.

The Glauber approximation[14] may be viewed as an extension of the Born approximation into the intermediate velocity region near the peak of the cross section. In the case of excitation of atomic hydrogen to low-lying levels, the Glauber predictions give better agreement with observed results[17] than the simpler Born predictions as expected. At high projectile velocities, the Glauber approximation reduces to the Born approximation, e.g., at 200 keV, Glauber predictions for excitation by protons of atomic hydrogen from $n=1$ to $n=2$ lie 8% below the Born predictions.

The total cross section for the ionization of atomic hydrogen by proton impact may be expressed in terms of the square of the scattering amplitude, i.e.,

$$\sigma(k_0)=2k_0^{-2}\int |f(q,\vec{k})|^2 q\,dq\,k^2 dk\,d\Omega_k \quad (\pi a_0^2), \tag{5}$$

in which $\vec{k}_0$ is the momentum of the projectile, $\vec{q}$ is the momentum transfer, a_0 is the Bohr radius, and $\vec{k}$ is the momentum of the ejected electron. In the Glauber approximation, the scattering amplitude may be expressed[23] by

$$f_G(q,\vec{k})=\frac{ik_0}{2\pi}\int e^{i\vec{q}\cdot\vec{B}}\,u_f^*(\vec{r}) \times\left[1-\left(\frac{|\vec{B}-\vec{s}|}{B}\right)^{2i\eta}\right]u_i(\vec{r})\,d^3r\,d^2B, \tag{6}$$

in which $\eta=\mu/k_0=1/v_0$ is the reciprocal of the projectile velocity, u_i and u_f are the initial and final electron states, $\vec{R}=\vec{B}+\vec{Z}$ is the projectile coordinate, and $\vec{r}=\vec{s}+\vec{z}$ is the electron coordinate with $\vec{q}\cdot\vec{Z}=0$. In keeping with Born calculations of direct Coulomb ionization, $u_f(\vec{r})$ is chosen to be a Coulomb wave function. This corresponds to the widely used screening approximation[23] in which one assumes that the ejected electron leaves the target at a slower speed than the projectile so that the remaining target charge is completely screened from the projectile by the ejected electron. This approximation for the continuum wave function may break down when the velocity of the ejected electron is comparable to the velocity of the projectile.

The above expression for the Glauber ionization amplitude may be reduced to a one-dimensional numerical integral[18,24,25] by expanding the amplitude in partial waves of the outgoing electron, corresponding to

$$f(q,\vec{k})=\sum_{l=0}^{\infty}\sum_{m=-l}^{l} f_{lm}(q,k)Y_l^m(\hat{k}). \tag{7}$$

By using the orthonormality of the spherical harmonics, the expression for the differential cross section as a function of the momentum of the ejected electron is found from Eq. (5) to be

$$\frac{d\sigma}{dk}=\frac{2k^2}{k_0^2}\sum_{l,m}\int |f_{l,m}(q,k)|^2 q\,dq. \tag{8}$$

In our calculations, we have followed the work of Golden and McGuire[18] to compute differential cross sections, $d\sigma/dk$, in the Glauber approximation. We have included partial waves for $l\leq 4$. For ejected electron momenta of $k=1.67$ (atomic units) that correspond to the largest observed

TABLE I. Coefficients A_m obtained by fitting with Eqs. (3) and (4). ξ is expressed in eV and $d\sigma/d\xi$ in cm^2/eV. The approximate relationship, $d\sigma(\xi)/d\xi\approx\sum_m A_m\xi^{-m}$, is not valid for $\xi<13.6$ eV.

E (keV)	$A_{3.5}$	$A_{4.5}$	$A_{5.5}$	$A_{6.5}$	$A_{7.5}$	$A_{8.5}$
25		1.83×10^{-11}	-1.39×10^{-10}	-1.35×10^{-9}	-6.37×10^{-8}	9.16×10^{-7}
50	2.76×10^{-12}	-9.66×10^{-11}	1.60×10^{-9}	-1.63×10^{-8}	8.43×10^{-8}	
75	2.20×10^{-12}	-5.82×10^{-11}	4.28×10^{-10}			
145	7.07×10^{-13}	-1.64×10^{-11}	1.16×10^{-10}			
200	6.20×10^{-13}	-1.50×10^{-11}	1.14×10^{-10}			

value, our numerical error is estimated at about 15% primarily as a result of the truncation past $l=4$. At $k<1.0$, our numerical error is estimated to be less than 5%. Our theoretical cross sections, $d\sigma/dk$, are related to the observed energy-loss spectra by observing that the energy lost by the incident proton, ξ, is related to the energy gained by the atomic electron $k^2/2$, by $\xi = 1/2 + k^2/2$ in atomic units. Because $d\xi = k\,dk$, the ionization energy-loss cross section corresponds to

$$\frac{d\sigma}{d\xi} = \frac{1}{k}\frac{d\sigma}{dk} . \tag{9}$$

Integration of both the Glauber and Born differential cross sections over all ejected electron momenta yields total cross sections that are in agreement with previous[18] calculations.

COMPARISON OF EXPERIMENT AND THEORY

Figure 2 shows the experimental and theoretical differential cross sections. The theoretical curves for the Glauber approximation and Born approximation are from the present calculations. The binary encounter calculation curves are from the work of Garcia.[13] A Born calculation by Bell *et al.*[12] is available but not shown.

The theoretical curves in Fig. 2 fall off more rapidly with increasing energy loss than the data. This effect is most marked in the 25-keV differential cross section curves. Here the Born approximation curve is higher than the data near the ionization threshold and decreases more rapidly with increasing energy loss than the experimental data. The Glauber approximation also falls off more rapidly than the experimental data near the ionization threshold. Also the Glauber calculation is lower in magnitude than the data at all energies. The difference in absolute magnitude between all the theories and experiment decreases with increasing projectile energy. Even at 25 keV, the theories and experiment appear to converge at large energy losses.

The differential cross section data shown in Fig. 2 are similar but not identical in shape. The 25-keV differential cross section shows a region between 15 and 25 eV energy loss that is definitely less curved than the same region in the other differential cross section curves. This effect is not reproduced by the theoretical curves. The theoretical curves, however, reproduce the curve shape of the 200-keV data quite well.

Several explanations for the breakdown of the theory are possible. These include trajectory corrections,[26] binding energy and recoil corrections,[27] and possible cumulative effects brought about by mathematical simplification and truncation.[28] However, we ascribe the discrepancy to charge transfer to the continuum,[3,29,30] in which the ejected electron is swept into a continuum state of the projectile. In our Glauber and Born approximations, the ejected electron is considered to be in a continuum state of the target with the projectile treated as a plane wave. This description is not adequate to describe properly those electrons that are ejected with velocities comparable to the velocity of the scattered proton.

The continuum charge transfer process has been noted in several measurements of the angular distribution of ejected electrons[3,29] and has been discussed in several theoretical papers.[30-34] Kim[34] has suggested the use of a Platzman plot to display features in $d\sigma/d\xi$ that represent collision mechanisms other than simple ionization. In a Platzman plot, the ratio of the experimental cross section to the Rutherford cross section for the outermost orbital, i.e.,

$$Y(\xi, T) = \frac{d\sigma}{d\xi}\,\frac{T}{4\pi a_0^2 Z^2}\,\frac{\xi^2}{\xi_0^2} , \tag{10}$$

is plotted as a function of ξ_0/ξ. In this equation, ξ_0 is equal to 13.6 eV, a_0 is the Bohr radius, and T is equal to $m_e V^2/2$ expressed in eV. Here, m_e is the mass of the electron, Z is the charge of the incident projectile, and V is the projectile velocity.

Platzman plots for the continuum portion of the energy-loss spectra for 25 and 50 keV protons incident on atomic hydrogen are shown in Fig. 3. In this figure, arrows indicate the kinetic energy of electrons ejected with the same speed as that of the incident proton. The broad peak seen in the Platzman plot is located at energies about 10% less than the kinetic energy of electrons ejected with the same speed as the scattered proton. This distribution is consistent with expectations for an electron undergoing a charge transfer to a continuum state of a hydrogen atom.[34]

Figure 3 also shows the Glauber and Born approximation differential cross sections. The theoretical curves are smooth and slowly decrease with decreasing values of ξ_0/ξ. Particularly in the case of 25-keV curves, the theory and experiment appear to approach one another at small values of ξ_0/ξ.

When proton impact spectra and electron impact spectra are displayed on Platzman plots, the proton data are dominated by the broad continuum charge transfer peaks, which do not have counterparts on the electron impact data. These observations suggest that charge transfer may be considered an additional electron production process in our case rather than a redistribution of slow ejected electrons.[34]

None of our theoretical treatments of direct

Coulomb ionization properly include the continuum charge transfer process. The charge transfer to the continuum contributions are expected to be large in the portion of the ejected electron spectra when the contributions from direct Coulomb ionization calculations are small. Thus the Glauber and Born predictions should be lower than the experimental measurements, which do include electrons from the process. In our observations, the contribution to the cross section, which is attributable to the continuum charge transfer process, could be as high as 20%. Because the ejected electrons are in the continuum, continuum charge transfer is part of the overall ionization cross section. Hence, in principle, the process should not be studied independently of ionization.

The effect of charge transfer to the continuum is less striking at high impact energies. The effect is still present, only it is distributed over a larger range of energy losses. With this in mind, agreement with theory at 200 keV must be considered good because of the similarity of the curve shapes. The experiment is slightly higher than theory as would be expected, both because of the additional contribution from the continuum charge transfer process and because of our normalization to the Born rather than the Glauber excitation cross section as discussed below.

Figure 4 shows the results of integrating the data to obtain ionization cross sections. The triangles represent our data normalized as described. The solid circles represent the data of Gilbody and Ireland,[1] and the solid squares represent the data of Fite *et al.*[2] Both of these latter measurements were made by using crossed-beam techniques. They were normalized by measuring the ratio of the cross section for ionization of atomic hydrogen to that of molecular hydrogen. The cross sections were made absolute by comparing them with the accepted value of the cross section for the ionization of molecular hydrogen. Our data are higher than the data of Gilbody and Ireland. The one point at 25 keV is in good agreement with the data of Fite's group. The experimental arrangement used

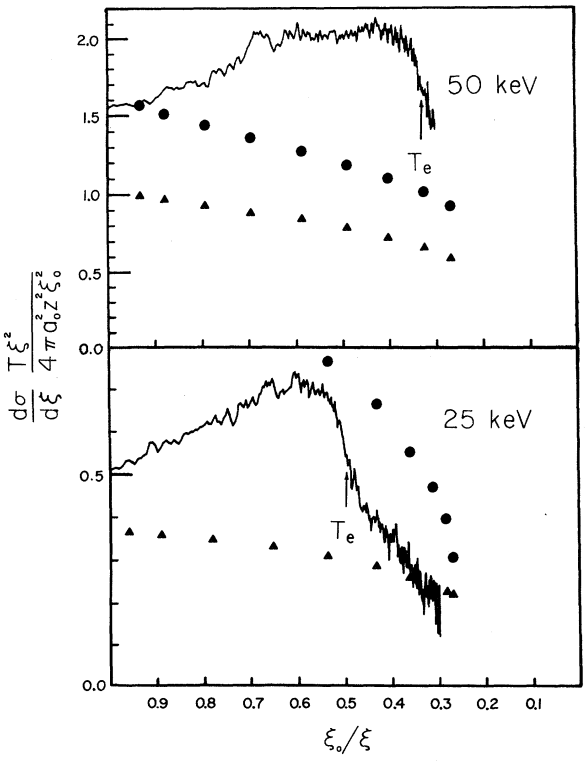

FIG. 3. Platzman plot for the ionization continuum of atomic hydrogen under proton impact. The heavy lines are the corrected normalized data. The solid circles are due to the Born approximation calculations. The solid triangles represent our Glauber calculations. The arrows indicate the kinetic energy of electrons ejected with the same speed as that of the incident protons.

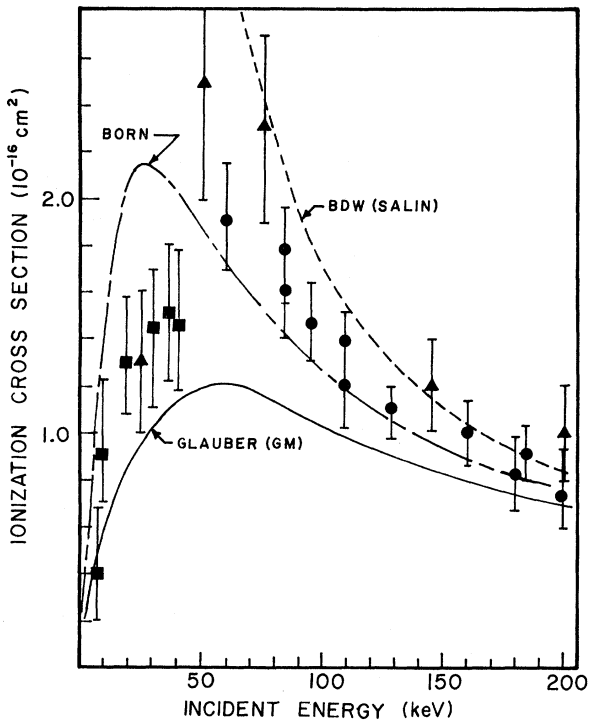

FIG. 4. Ionization cross section for atomic hydrogen under proton bombardment. The solid squares are the data of Fite *et al.* (Ref. 2). The solid circles are the data of Gilbody and Ireland (Ref. 1). The solid triangles are our data from spectra that were normalized to the Born approximation cross section for excitation of atomic hydrogen to the $n=2$ state. Both the Born approximation (B) and Glauber approximation (GM) cross sections were taken from Golden and McGuire (Ref. 18). The Born distorted wave (BDW) approximation cross sections were taken from Salin (Ref. 35).

by Gilbody and Ireland and Fite *et al.* should have included the charge transfer to the continuum electrons in the ionization current measurement. Considering the major differences between the two techniques, the agreement between the energy-loss and crossed beam experiments is very good. Figure 4 also shows the Golden and McGuire[18] calculations in the Born and Glauber approximations. The data are higher than either theoretical curve; however, this result should be expected because neither theory includes contributions from charge transfer to the continuum.

A calculation by Salin,[35] in which the interaction between the ejected electron and the scattered proton are explicitly included, is also shown. In this Born distorted wave calculation, the Coulomb fields of both the projectile and target protons are considered. The long-range interaction between the ejected electron and the scattered proton enhances the cross section when the velocities of the ejected electron and the incident proton are equal. The results of this calculation are markedly higher than the Born or Glauber cross section curves. The agreement with the data is good at impact energies greater than 75 keV. For energies less than 75 keV, the theoretical curve is much higher than the experimental results. The contribution of the long-range interaction in this theory appears to be of the right magnitude. Overestimation of the cross section at the low energies is typical of Born approximation calculations and is not necessarily a result of the inclusion of the long-range effects in the theory.

DISCUSSION

The data presented here represent the first measurements of the energy differential cross section $d\sigma/d\xi$ for the ionization by proton bombardment of atomic hydrogen. The agreement with other total ionization cross section measurements and with theory is very good.

The data have been normalized by using the Born calculation of the cross section for the excitation of atomic hydrogen to the $n=2$ state (σ_2) by 200 keV protons. The choice of normalizing to the Born approximation calculation was made at the time of the preliminary publication of the σ_2 data,[5] and this normalization has been retained for consistency. The best fit to the excitation data is given by the Glauber approximation calculations.[17,36,37] Also, comparison with proton-helium collisions[38,39] indicates that the Glauber approximation calculations are reliable at lower proton impact energies than Born approximation calculations. These considerations suggest that it might have been better to normalize to the Glauber calculation; however, the reader may easily renormalize the data by multiplying the results by 0.9218. It must be noted that renormalization to the Glauber approximation calculation would lower the data by 8% and thus improve both the fit to the theory and the agreement with the data of Gilbody and Ireland.

The comparison of the data and theory for the differential cross section of atomic hydrogen emphasizes the breakdown of the Glauber and Born theories of direct Coulomb ionization by proton impact. This difference between theory and experiment is dramatically demonstrated in the Platzman plots. The same plots indicate that this effect is an additional contribution to the ionization. Additional theoretical effort is required to describe in a quantitative manner collisional ionization by proton impact even for simple targets, such as atomic hydrogen.

---

*Work supported by the National Science Foundation.
†Supported in part by the U. S. Energy Research and Development Administration under Contract No. E(11-1)-2753.

[1]H. B. Gilbody and J. V. Ireland, Proc. R. Soc. 277, 137 (1963).
[2]W. L. Fite, R. F. Stebbings, D. G. Hummer, and R. T. Brackmann, Phys. Rev. 119, 663 (1960).
[3]M. E. Rudd, Radiat. Res. 64, 153 (1975).
[4]L. H. Toburen and W. E. Wilson, *Abstracts of the Eighth International Conference on the Physics of Electronic and Atomic Collisions, Belgrade, 1973,* edited by B. C. Čobić and M. V. Kurepa (Institute of Physics, Belgrade, 1973), p. 693.
[5]J. T. Park, J. E. Aldag, and J. M. George, Phys. Rev. Lett. 34, 1253 (1975).
[6]J. T. Park and F. D. Schowengerdt, Rev. Sci. Instrum. 40, 753 (1969).
[7]V. Pol, W. Kauppila, and J. T. Park, Phys. Rev. A 8, 2990 (1973).
[8]G. W. York, Jr., J. T. Park, J. J. Miskinis, D. H. Crandall, and V. Pol, Rev. Sci. Instrum. 43, 230 (1972).
[9]F. D. Schowengerdt and J. T. Park, Phys. Rev. A 1, 848 (1970).
[10]V. Pol, J. George and J. T. Park, Bull. Am. Phys. Soc. 18, 1517 (1973).
[11]D. R. Schoonover and J. T. Park, Phys. Rev. A 3, 228 (1971).
[12]K. L. Bell, M. W. Freeston, and A. E. Kingston, J. Phys. B 3, 959 (1970).
[13]J. D. Garcia, Phys. Rev. 177, 223 (1969).
[14]E. Gerjuoy and B. K. Thomas, Rep. Prog. Phys. 37, 1345 (1974).
[15]J. E. Golden and J. H. McGuire, Phys. Rev. Lett. 32,

1218 (1974).
[16]H. Narumi, A. Tsuji, and A. Miyamoto, *Proceedings of the Fourth International Conference on Atomic Physics, Abstracts of Contributed Papers, Heidelberg, 1974,* edited by J. Kowalski and H. G. Weber (Heidelberg U.P., Heidelberg, 1974), p. 398.
[17]J. T. Park, J. E. Aldag, J. M. George, and J. L. Peacher, Phys. Rev. A 14, 608 (1976).
[18]J. E. Golden and J. H. McGuire, Phys. Rev. A 12, 80 (1975).
[19]R. Abrines and I. C. Percival, Proc. Phys. Soc. (London) 88, 873 (1966).
[20]K. Omidvar, Phys. Rev. 140, A26 (1965).
[21]E. Merzbacher and H. W. Lewis, *Encyclopedia of Physics* (Springer-Verlag, Berlin, 1958), Vol. 34, p. 166.
[22]D. R. Bates and G. Griffing, Proc. Phys. Soc. A66, 961 (1953).
[23]J. H. McGuire, M. B. Hidalgo, G. D. Doolen, and J. Nuttall, Phys. Rev. A 7, 973 (1973).
[24]H. Narumi, A. Tsuji, and A. Miyamoto, Prog. Theor. Phys. 54, 740 (1975).
[25]B. K. Thomas, Bull. Am. Phys. Soc. 19, 1191 (1974) and private communication.
[26]F. W. Byron [Phys. Rev. A 4, 1907 (1971)] computes corrections to the Glauber approximation which are small for excitation of atomic hydrogen by electron impact but which significantly raise the cross sections for excitation by positron impact.
[27]J. F. Reading, Phys. Rev. A 1, 1642 (1970).
[28]B. K. Thomas, Bull. Am. Phys. Soc. 20, 1467 (1975). Thomas suggests checking convergence for very large l of Eq. (8).
[29]J. B. Brooks and M. E. Rudd, Phys. Rev. A 3, 1628 (1972).
[30]K. Dettmann, K. C. Harrison, and M. W. Lucas, J. Phys. B 7, 269 (1974).
[31]J. Macek, Phys. Rev. A 1, 235 (1970).
[32]A. Salin, J. Phys. B 5, 979 (1972).
[33]Y. B. Band, J. Phys. B 7, 2557 (1974).
[34]Y. K. Kim, Radiat. Res. 64, 96 (1975).
[35]A. Salin, J. Phys. B 2, 631 (1969).
[36]V. Franco and B. K. Thomas, Phys. Rev. A 4, 945 (1971).
[37]K. Bhadra and A. S. Ghosh, Phys. Rev. Lett. 26, 737 (1971).
[38]R. Hippler and K. H. Schartner, J. Phys. B 7, 618 (1974).
[39]C. J. Joachain and R. Vanderpoorten, J. Phys. B 7, 817 (1974).